

Membrane Simulations of OpcA: Gating in the Loops?

Peter J. Bond,* Jeremy P. Derrick,[†] and Mark S. P. Sansom*

*Department of Biochemistry, University of Oxford, Oxford, United Kingdom; and [†]Faculty of Life Sciences, University of Manchester, Manchester, United Kingdom

ABSTRACT Mobility of extracellular loops may play an important role in the function of outer membrane proteins from Gram-negative bacteria. Molecular dynamics simulations of OpcA from *Neisseria meningitidis*, embedded in a lipid bilayer, have been used to explore the relationship between the crystal structure and dynamic function of this protein. The results suggest that the crystal environment may constrain the membrane protein structure in a nonphysiological state. The presence of lipids and physiological salt concentrations result in changes in the conformation of the extracellular loops of OpcA, leading to opening of a pore, and to modulation of the molecular surface implicated in recognition of proteoglycan. These changes may be related to the role of OpcA in pathogenesis via modulation of the conformation of a possible sialic acid binding site.

Received for publication 13 September 2006 and in final form 7 November 2006.

Address reprint requests and inquiries to Mark S. P. Sansom, Tel.: 44-1865-275371; Fax: 44-1865-275273; E-mail: mark.sansom@bioch.ox.ac.uk.

Progress in structural biology has yielded ~110 distinct high resolution membrane protein structures. However, it appears that the experimental conditions under which a membrane protein structure is obtained, e.g., presence of detergent/lipid (1), crystallization solutes (2), or pH (3), may influence aspects of its conformation. This is important when trying to relate (static) structure to (dynamic) biological function. Molecular dynamics (MD) simulations yield dynamic information on membranes (4). MD is used here to investigate loop mobility in relation to ligand binding and the possibility of channel gating in the outer membrane protein (OMP) OpcA. OpcA is an adhesion protein from *Neisseria meningitidis* implicated in the development of meningitis and septicemia in humans. OpcA is thought to mediate attachment to host cells by binding proteoglycan cell-surface receptors. Its x-ray structure (5) shows that OpcA forms a 10-stranded β -barrel, with five highly mobile extracellular loops. The loops form a positively charged crevice that could theoretically accommodate proteoglycan. However, fluorescence-based binding studies suggest the binding site may be in a different location, near to a tyrosine residue (Tyr-169) adjacent to residues in loop L2 (6). Moreover, whereas the β -barrel interior of OpcA is water-filled and rather wide (mean radius ~0.2 nm), loop L2 adopts an unusual conformation, traversing the barrel axis and thereby preventing formation of a continuous pore.

Thus, the conformation of the loops is important in understanding both the mechanism of host cell adhesion and the possibility of pore formation by OpcA. Zn^{2+} ions were necessary for formation of OpcA crystals. Crystallographic densities for three such ions were identified in the structure, one within the central cavity in the interior of the β -barrel and two on the extracellular surface in the loops that mediate crystal packing interactions. It is therefore of interest to establish how more “physiological” conditions might alter the

conformation of the protein. Thus, two 20 ns MD simulations were carried out for OpcA in a lipid (dimyristoyl-phosphatidylcholine) bilayer, in either ~0.1 M or ~1 M NaCl (Fig. 1). (Details in Supplementary Material.)

The C^α root mean-squared deviation (RMSD) allows the measurement of the drift of the protein from its initial crystal-derived conformation (Fig. 2). In both simulations, the β -barrel domain of OpcA proved to be particularly stable, with the RMSD peaking at to 0.15–0.2 nm within ~5 ns. In contrast, the extracellular loops showed much greater conformational drift, with an RMSD of ~0.4 nm within the first ~5 ns, and final values reaching 0.4–0.45 nm by 20 ns. Consistent with its length and lack of defined structure, loop L2 seemed to be the primary contributor to this high RMSD, with localized sections exhibiting large twisting motions, as indicated by principal component analysis.

The large RMSD in the extracellular loops appears to be a result of the absence of Zn^{2+} ions and crystal-packing contacts. Specifically, the side chains of residues Asp-69, His-128, and Thr-176 (in loops L2, L3, and L4, respectively) and Glu-223 (in loop L5 of an adjacent monomer) were within 0.35 nm of one Zn^{2+} ion. Moreover, a salt-bridge is present between the L5 loops of adjacent monomers. Visual inspection of the simulations indicated significant conformational changes in these loop regions. Two small α -helices in loops L2 and L4 completely (0.1 M simulation) or partly (1 M simulation) unfolded (Fig. 3), whereas a small β -strand section in L2 formed in the 0.1 M system. Moreover, these changes were propagated to loop L5, where a small β -hairpin grew by a few residues. The higher ion concentration seems in part to stabilize the crystallographic-induced loop structure in comparison with the 0.1 M simulation. This was

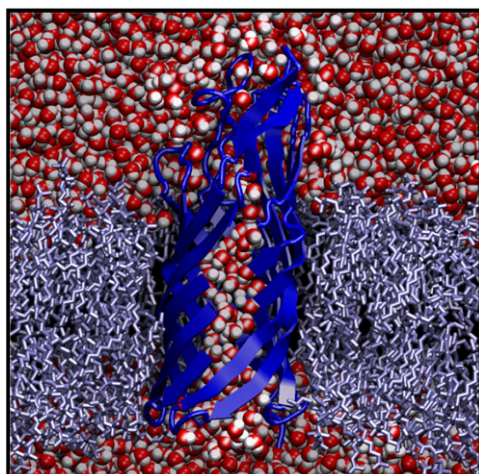


FIGURE 1 Snapshot of OpcA (cutaway *blue* cartoon format) within a dimyristoyl-phosphatidylcholine bilayer (*light blue*) surrounded by water (*red/white*), with ions omitted for clarity.

confirmed by calculating the simulated C^α B-factors, which showed consistently higher loop fluctuations for the 0.1 M simulation. Although the highest region of mobility in the protein for each simulation was observed in loop L2, each peaking around Gly-74, which lies at the tip of the loop, the relative magnitude is significantly greater for the 0.1 M simulation ($\sim 300 \text{ \AA}^2$) than the 1 M simulation ($\sim 50 \text{ \AA}^2$). The difference may arise from a greater extent of ionic interactions with charged residues in the loops of OpcA (L2 alone contains six Lys residues and four Asp/Glu residues).

Thus, it appears that whereas the Zn^{2+} ion and crystal contacts hold loops L2 and L4 together, they concurrently induce a possibly nonnative α -helical conformation. What impact might this have on our interpretation of the biological function of OpcA? In the simulations, the L1, L2, and L5 loop regions undergo significant changes in conformation, leading to changes in the crevice feature identified in the original OpcA structure. This site effectively closes off completely (in the 0.1 M simulation) or partially (in the 1 M simulation) (Fig. 3). On the other hand, in the crystal structure, two Pro residues (Pro-82 and Pro-86) in L2 lead to a tapering of the pore, due to a kink in the loop that covers the mouth of the barrel, before extending outward at a second

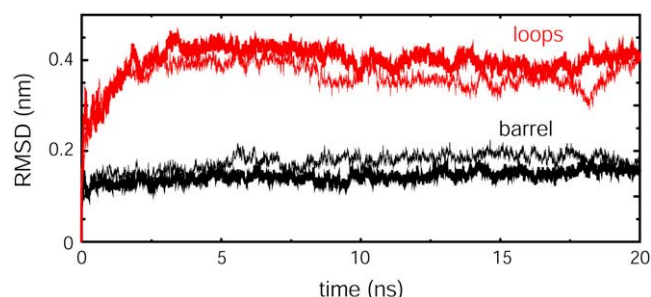


FIGURE 2 C^α RMSD in the 0.1 M (*thick lines*) and 1 M (*thin lines*) simulations for the barrel and extracellular loops.

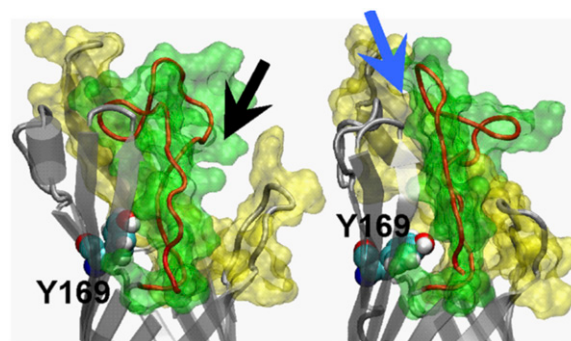


FIGURE 3 Snapshots of the extracellular surface of OpcA (*gray* cartoon format) for the crystal structure (*left*) and at 20 ns for the 0.1 M MD simulation (*right*). In the crystal, a crevice (*black arrow*) is formed primarily between loop L2 (*red* cartoon format surrounded by its *green* molecular surface) and loops L1 and L5 (*yellow* molecular surface). Motions in loop L2 and L5 result in the closure of this cleft and the formation of a pathway (*blue arrow*) from the solvent to Tyr-169 (space-filling format).

kink (Fig. 4). It is noteworthy that residues Lys-80 to Thr-83 in loop L2 lie adjacent to Tyr-169 (Fig. 3), which plays a major role in the intrinsic fluorescence response to sialic acid binding (6). During simulation, the induced closure of the extracellular loop crevice is accompanied by the movement of L2 away from the barrel mouth and Tyr-169, supported by conformational changes in the tip of L1. Biologically, this may represent the first stage in the creation of a pathway required for binding proteoglycan receptors.

The two Pro residues in loop L2, along with the Glu-70/Lys-72 salt bridge at the tip of the loop (Fig. 4), result in the pore radius of OpcA being reduced to a minimum of $\sim 0.02 \text{ nm}$ at the mouth of a putative channel through OpcA. In contrast, the observed conformational changes in the loops during simulation result in a significant widening of the barrel mouth. In particular, at the main block to pore formation, at Pro-82, the radius in both simulations is increased to $\sim 0.1 \text{ nm}$ on average over the final 15 ns, and the large fluctuations in pore radius along the whole length of loop L2 mean that the entire barrel mouth is significantly opened in comparison with the

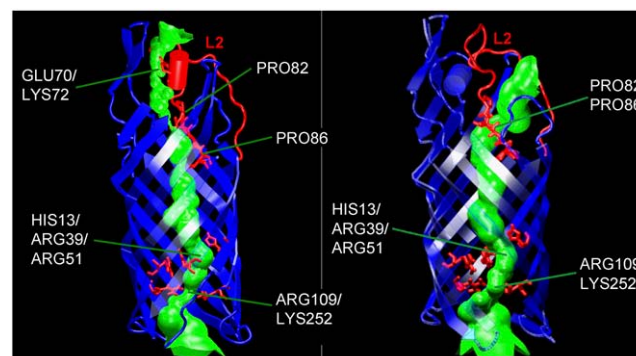


FIGURE 4 Internal pore surface (*green*) (analyzed using HOLE (7)) for the crystal structure (*left*) and open 0.1 M simulation (*right*). Residues in L2 (*red*) and the barrel are indicated.

crystal structure. Consequently, a continuous pore can be found along the length of the protein for long periods of each simulation (Fig. 4). This is formed beyond the Arg-109/Lys-252 pair at the intracellular mouth, through the His-13/Arg-39/Arg-51 triad, and out of the now widened extracellular mouth, past the pair of Pro residues and through the center of L2.

It should be noted that no ions were observed to pass through the pore in either simulation, as the simulation time is likely to be an order of magnitude lower than the time required for the diffusion of a single ion through a transmembrane pore. Nevertheless, multiple water molecules were observed to traverse the length of the pore, bypassing the pair of Pro residues that originally blocked the barrel mouth in the crystal structure. For comparison, a short (7 ns) simulation was performed, in which the loop residues involved in coordinating the Zn^{2+} ion were restrained relative to one another. Despite these restraints, significant changes in the surrounding loop regions were observed (see Supplementary Material), enabling a few water molecules to pass through the pore. This suggests that the crystal contacts between loops of adjacent OpcA monomers help to maintain the conformation of loop L2.

It should be noted that OpcA has not been reported to form ion permeable pores. However, assuming that OpcA is filled with a 1 M KCl solution, based on the simulated pore size, the conductance of a putative OpcA channel was predicted to be ~ 100 pS (7). Interestingly, the minimum pore radius fluctuates significantly on a nanosecond timescale due to the Pro kinks in loop L2, leading to variation in predicted conductance over each simulation of between ~ 0 and 250 ps. Similar flickering patterns of conductance have also been observed via simulated (8) and experimental (9) measurements for OmpA.

The simulation study presented here reveals that the absence of crystal-packed neighboring proteins and Zn^{2+} ions, and the presence of a more biologically relevant bilayer, result in concerted conformational changes in the extracellular loops. These loop motions result in the unblocking of the pore toward the extracellular mouth of the β -barrel, as well as rearrangement of external surface of OpcA. The simulations indicate that the ligand binding site may be quite dynamic, suggesting the possibility of an induced fit mechanism. The movement of loop L2 away from Tyr-169 is supportive of a mechanism in vivo whereby conformational changes in the extracellular loops precede proteoglycan binding. Interestingly, raising the salt concentration in our simulations resulted in higher protein stability and a consequent moderation of these effects. This is pertinent in the light of recent crystal structures of a 14-stranded β -barrel protein, OmpG (3). The study revealed that the pH gated opening of its pore is effected via structural changes in a long extracellular loop, which is folded across the barrel in the closed state only. Moreover, Gd^{3+} ions have been shown to close OmpG (10), whereas Ca^{2+} ions were observed to bind to the extracellular loops. Similarly, in plant aquaporins, a loop blocks the channel from the cytoplasm but upon displacement opens the pore (11). Binding of divalent cations near this gating loop

has been implicated in regulation. It therefore seems feasible that sensing the local environment via structural changes in extracellular loops may be a common theme for membrane proteins. In the case of OpcA, this may affect ligand binding, thereby aiding the correct identification of specific host sites for successful adhesion of *N. meningitidis* cells, the first step in the pathogenesis of disease. This is especially important as OpcA needs to recognize the sialic acid on the surface of epithelial cells while surrounded by a “sea” of lipopolysaccharide rich in sialic acid in the bacterium’s own outer membrane surface. It will therefore be of interest to extend simulations of OpcA and other outer membrane proteins to a model of the environment provided by the lipopolysaccharide of Gram-negative bacterial outer membranes (12).

SUPPLEMENTARY MATERIAL

An online supplement to this article can be found by visiting BJ Online at <http://www.biophysj.org>.

ACKNOWLEDGEMENTS

This work was supported by the Biotechnology and Biological Sciences Research Council, the Membrane Protein Structure Initiative consortium (www.mpsi.ac.uk), and the Wellcome Trust.

REFERENCES and FOOTNOTES

1. Lee, A. G. 2005. How lipids and proteins interact in a membrane: a molecular approach. *Molec. Biosys.* 1:203–212.
2. Kim, M., Q. Xu, G. E. Fanucci, and D. S. Cafiso. 2006. Solutes modify a conformational transition in a membrane transport protein. *Biophys. J.* 90:2922–2929.
3. Yildiz, O., K. R. Vinothkumar, P. Goswami, and W. Kühlbrandt. 2006. Structure of the monomeric outer-membrane porin OmpG in the open and closed conformation. *EMBO J.* 25:3702–3713.
4. Bond, P. J., and M. S. P. Sansom. 2004. The simulation approach to bacterial outer membrane proteins. *Mol. Memb. Biol.* 21:151–162.
5. Prince, S. M., M. Achtman, and J. P. Derrick. 2002. Crystal structure of the OpcA integral membrane adhesin from *Neisseria meningitidis*. *Proc. Natl. Acad. Sci. USA.* 99:3417–3421.
6. Moore, J., S. E. S. Bailey, Z. Benmechemene, C. Tzitzilonis, N. J. E. Griffiths, M. Virji, and J. P. Derrick. 2005. Recognition of saccharides by the OpcA, OpaD, and OpaB outer membrane proteins from *Neisseria meningitidis*. *J. Biol. Chem.* 280:31489–31497.
7. Smart, O. S., J. Breed, G. R. Smith, and M. S. P. Sansom. 1997. A novel method for structure-based prediction of ion channel conductance properties. *Biophys. J.* 72:1109–1126.
8. Bond, P. J., J. D. Faraldo-Gómez, and M. S. P. Sansom. 2002. OmpA: a pore or not a pore? Simulation and modeling studies. *Biophys. J.* 83:763–775.
9. Hong, H., G. Szabo, and L. K. Tamm. 2006. Electrostatic couplings in OmpA ion-channel gating suggest a mechanism for pore opening. *Nat. Chem. Biol.* 2:627–635.
10. Conlan, S., Y. Zhang, S. Cheley, and H. Bayley. 2000. Biochemical and biophysical characterization of OmpG: a monomeric porin. *Biochem.* 39: 11845–11854.
11. Tornroth-Horsefield, S., Y. Wang, K. Hedfalk, U. Johanson, M. Karlsson, E. Tajkhorshid, R. Neutze, and P. Kjellbom. 2006. Structural mechanism of plant aquaporin gating. *Nature.* 439:688–694.
12. Lins, R. D., and T. P. Straatsma. 2001. Computer simulation of the rough lipopolysaccharide membrane of *Pseudomonas aeruginosa*. *Biophys. J.* 81:1037–1046.